

Investigating the reduction in the absorption intensity of P3HT in polymer/fullerene “bilayers” coated using orthogonal solvents

Chunmei Zhang,^{1,2} Yufeng Hu,¹ Aiwei Tang,¹ Zhenbo Deng,¹ Feng Teng¹

¹Institute of Optoelectronic Technology, Beijing JiaoTong University, Beijing 100044, China

²Beijing Institute of Graphic Communication, Beijing 102600, China

Correspondence to: Y. Hu (E-mail: yfhu@bjtu.edu.cn) and F. Teng (E-mail: fteng@bjtu.edu.cn)

ABSTRACT: We investigated the reduction in the absorption intensity of poly(3-hexylthiophene) (P3HT) in a poly(3-hexylthiophene)/(6,6)-phenyl-C₆₁-butyric acid methyl ester (P3HT/PCBM) “bilayer” heterojunction film that was fabricated using orthogonal solvents. The results show that even though P3HT is insoluble in dichloromethane (DCM), DCM could decrease the chain packing and the crystallinity of the P3HT film by the swelling effect. DCM also assists in the penetration of the PCBM into the P3HT underlayer during spin-coating. After the DCM evaporates, the PCBM in the P3HT matrix hinders the self-reorganization of P3HT, causing a drop in the absorption intensity of P3HT. © 2014 Wiley Periodicals, Inc. *J. Appl. Polym. Sci.* **2015**, *132*, 41757.

KEYWORDS: blends; films; swelling

Received 14 July 2014; accepted 2 November 2014

DOI: 10.1002/app.41757

INTRODUCTION

Thin film organic photovoltaic (OPV) solar cells have attracted substantial scientific interest in the last decades because of their potential applications in lightweight, flexible, large-area, and low-cost electronics.^{1,2} Since the seminal work of Tang in 1986,³ two main methods have been explored to develop OPV devices: a planar heterojunction or a phase separated bulk heterojunction (BHJ). A planar bilayer structure was commonly achieved by depositing acceptor and donor thin films sequentially one after another. The planar bilayer structure limits the donor–acceptor interfacial area and the photons that are absorbed far away from the planar heterojunction are not able to yield charge carriers. Tang’s bilayer device based on copper phthalocyanine and a perylene tetracarboxylic derivative only exhibited a power conversion efficiency (PCE) of about 1%.³ And the PCE of the poly (3-hexylthiophene) (P3HT)/(6, 6)-phenyl-C₆₁-butyric acid methyl ester (PCBM) bilayer solar cell fabricated by stamping transfer and floatation method is only less than 0.6%.^{4,5} To increase the PCE values of the device, BHJ solar cells were developed to increase the donor–acceptor interfacial area. In a typical BHJ device, a blend film of a conjugated polymer donor and a fullerene derivative acceptor is fabricated to form a donor–acceptor interpenetrating network. The nanoscale interpenetrating network generates extreme donor/acceptor interfaces and so, the dissociation of excitons and the transport of the carriers are enhanced. Currently, most of efficient OPV solar cells are based on BHJ structure. The PCE over 9.2% has been

achieved for polymer-based solar cells with the BHJ architecture (based on PTB7 and PC₇₁BM system).⁶ Despite being outperformed by other material systems, P3HT and PCBM remain fundamental as an OPV benchmark.⁷ The PCE of a typical BHJ P3HT/PCBM device can approach 3~5% with optimizations such as thermal annealing, solvent annealing, adding chemical additives and inserting calcium cathodal interlayer.^{8,9}

Recently, Ayzner *et al.* demonstrated another type of all-solution-processed OPV cells.¹⁰ The active layer was deposited sequentially by spin-coating the *o*-dichlorobenzene (ODCB) solution of P3HT and the dichloromethane (DCM) solution of PCBM. DCM is regarded as an immiscible solvent for P3HT and has a negligible effect on the crystallinity of the P3HT film. Based on the neutron reflectivity measurement, the external quantum efficiency, X-ray photoelectron spectroscopy (XPS), time-of-flight secondary-ion mass spectrometry and the photoluminescence (PL) spectra, the researchers confirm that the PCBM diffuses into and mixes with the P3HT underlayer during the PCBM solution deposition and the annealing process, and the sequentially processed P3HT/PCBM film has a layer-evolved BHJ structure (LE-BHJ).^{11–15} Compared with the conventional planar and bulk heterojunctions (BHJs), the advantage of LE-BHJ structure is that it has an ideal vertical concentration profile for efficient photovoltaic devices. A PCBM-rich thin layer is close to the cathode and a P3HT-rich layer is close to the anode in the active layer, which reduces the charge recombination at anode/PCBM and cathode/P3HT interface and improves the

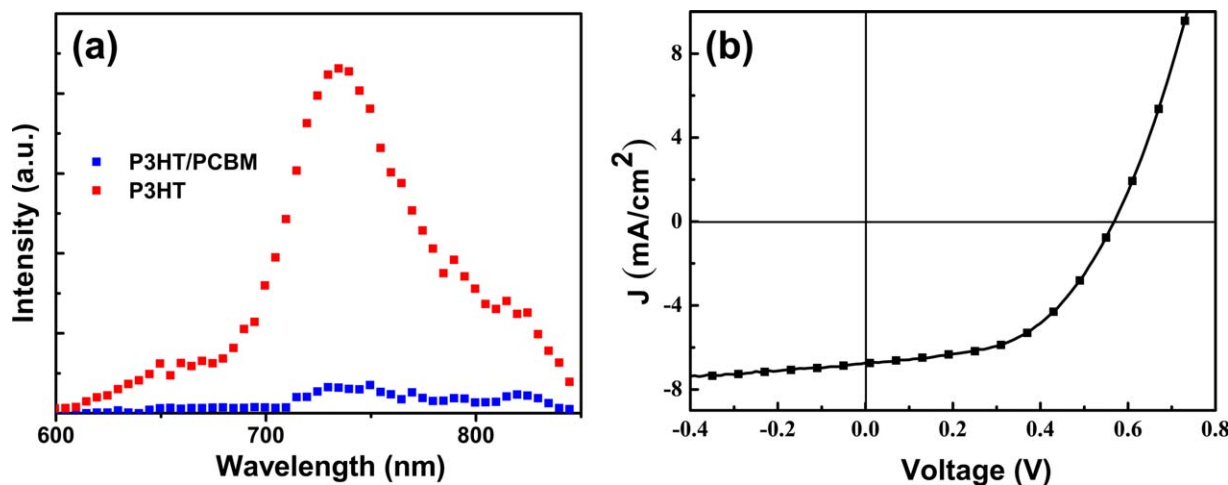


Figure 1. (a) The PL spectra of the pristine P3HT film and the P3HT/PCBM film. (b) The J–V curve of a layer-evolved BHJ device with the structure of ITO/PEDOT: PSS/P3HT/PCBM/Al. [Color figure can be viewed in the online issue, which is available at wileyonlinelibrary.com.]

PCE of the device. So far, many researchers have focused their attention on the improvement of the PCE of the LE-BHJ device. The studies demonstrate that the PCE of the device fabricated via sequential processing is comparable with or better than that of the conventional BHJ device.^{16–20}

The absorption spectra of P3HT, which are directly correlated with the interchain states and the degree of order in P3HT, have been widely used to characterize the morphological evolutions of P3HT in the conventional BHJ films. It is well established that the absorption intensity of P3HT is proportional to the P3HT chain packing and crystallinity.^{21–23} For the LE-BHJ P3HT/PCBM film, however, there are some controversies. On the one hand, the absorption intensity of P3HT/PCBM “bilayer” decreases significantly compared with the P3HT layer.¹³ On the other hand, the PCBM molecule is believed to be immiscible in the ordered P3HT, and the order of the P3HT crystalline domains of P3HT should be maintained with the interdiffusion of P3HT and PCBM.¹¹

In this work, we mainly investigate the relationship between the decrease of the absorption intensity and morphological change of P3HT during the PCBM diffusion, and try to understand the origins of the morphology evolution during process. From the absorption spectra and XRD patterns, we show that the P3HT film undergoes a swelling and deswelling process during the PCBM deposition process. DCM disturbs some of the crystalline domains of P3HT and the PCBM molecules in the DCM solution penetrate into these regions. Then PCBM molecules reside within the P3HT matrix after DCM evaporates, and hinder the re-organization of the P3HT. As a result, the order and the optical absorption of the P3HT decrease after the deposition of the PCBM layer. Therefore, this work is developing a better understanding of the origins and evolution of the morphology in the P3HT/PCBM layer, which is essential for improving the efficiency of polymer solar cells.

EXPERIMENTAL

P3HT and PCBM were obtained from Luminescence Tech. and FEM Tech., respectively. The dichlorobenzene (DCB) and DCM were purchased from Alfa Aesar. P3HT was washed in DCM for

several times before use. Then the dissolving of P3HT in the DCM can be regarded as negligible during the processes such as spin-coating, washing, and soaking etc.

The “bilayer” P3HT/PCBM films were fabricated as follows. First, the indium tin oxide (ITO) glass substrates were cleaned in an ultrasonic bath with a sequence of detergent, acetone and deionized water. The substrates were dried with N₂. The cleaned substrates were then placed in an ultraviolet-ozone generator for 5 minutes. Second, a thin layer of poly(3,4-ethylenedioxythiophene): poly(4-styrenesulfonate) (PEDOT: PSS) (30-nm thick) was spin-coated onto the substrate, and dried at 150 °C for 20 min in the oven. The P3HT solution with a concentration of 12 mg/mL in DCB was spin-coated on the top of PEDOT: PSS layer at 1000 rpm for 60 s. The thickness of the P3HT layer was about 80 nm. The sample was dried at 70 °C for 10 min. Then the 150 μL of PCBM solution with a concentration of 8 mg/mL in DCM was spin-coated on the top of P3HT layer at 800 rpm for 30 s. The thickness of the P3HT/PCBM film was about 110 nm in total. To fabricate the devices, an aluminium electrode (100-nm thick) was thermally deposited onto the P3HT/PCBM film. The anode and cathode together defined a device with an active area of 9 mm².

The thickness of the P3HT and P3HT/PCBM film was measured by a surface profilometer (Veeco Dektak 150). An ultraviolet–visible spectrophotometer (Shimadzu, uv-3101pc) and a fluorescence spectrometer (HORIBA JobinYvon, Fluorolog-3) were used to measure the absorption and PL spectra of the P3HT/PCBM films. The P3HT/PCBM films were prepared on the quartz substrates using the same methods that were used for the device fabrication. The crystallinity of P3HT was investigated by X-ray diffraction (Bruker, D8 advance) using Cu K α radiation ($\lambda = 0.15406$ nm). The photocurrent density–voltage (J–V) characteristics of the devices were recorded using a Keithley 4200 source measure unit. An AM 1.5 solar simulator (ABET Technologies) at 100 mW/cm² intensity was used to supply the illumination to the devices.

RESULTS AND DISCUSSION

Figure 1(a) shows the PL spectra of the pristine P3HT and the P3HT/PCBM films. The pristine P3HT film has an emission peak

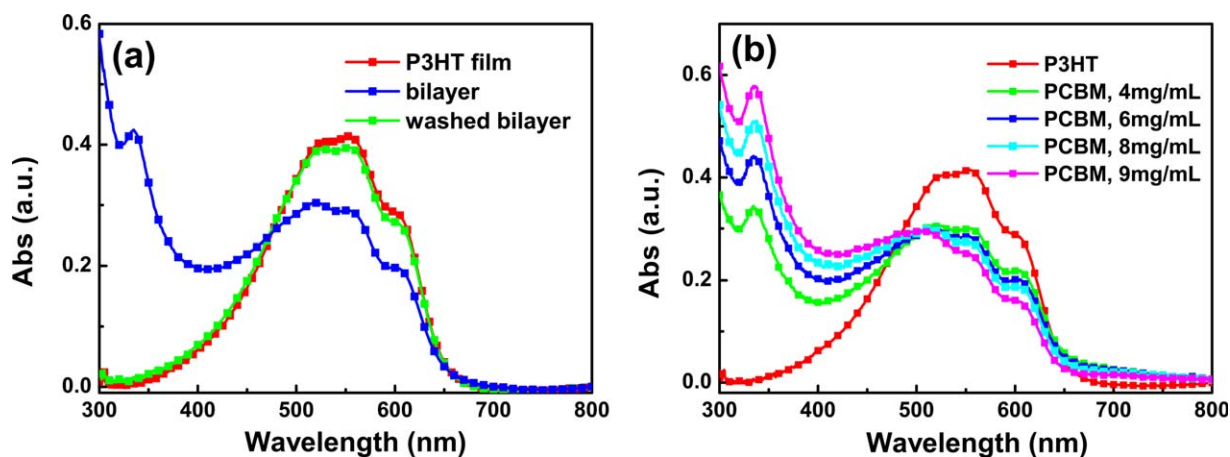


Figure 2. (a) The absorption spectra of the pristine P3HT film, the P3HT/PCBM film and the P3HT/PCBM film washed with DCM. (b) The absorption spectra of the P3HT film and the P3HT/PCBM films fabricated by spin-coating the PCBM solution on top of the P3HT from solutions that had different concentrations. The concentration of the PCBM solutions was varied from 4 to 9 mg/mL. [Color figure can be viewed in the online issue, which is available at wileyonlinelibrary.com.]

at 730 nm. The PL of P3HT in the P3HT/PCBM film is almost completely quenched. This indicates that there is sufficient PCBM in intimate contact with P3HT (within the excitation diffusion length, about 8~10 nm) and the excitons are successfully dissociated. Figure 1(b) shows the current–voltage characteristics of the solar cells with the device structure of ITO/PEDOT: PSS/P3HT/PCBM/Al. The active layer was fabricated by sequential, layer-by-layer spin-coating the DCB solution of P3HT and the DCM solution of PCBM. The device exhibits a PCE of 1.96%, with fill factor of 0.51%, open-circuit voltage of 0.57 V, and short-circuits current of 6.74 mA/cm². This PCE is much higher than the devices with the planar bilayer structure based on P3HT and PCBM.^{4,5} The fluorescence quenching and the high PCE of the device show that the LE-BHJ structure forms spontaneously during the deposition of PCBM. The effective intermixing of the P3HT and PCBM molecules offers a large heterojunction interface for efficient charge separation and gives rise to the efficient photovoltaic performance in the solar cells.

Figure 2(a) shows the absorption spectra of a P3HT film, a PCBM film, and a P3HT/PCBM film. The pristine P3HT film exhibits a broad peak. The main absorption peak is at 520 nm with two vibronic shoulder absorptions at 558 nm and 602 nm. This indicates strong interchain-interlayer interactions among the P3HT chains and high ordering of the polymer chains in the film.^{21–23} After spin-coating the PCBM on top of P3HT film, the absorption intensity of P3HT significantly decreases. The lower absorption intensity of P3HT in the LE-BHJ film is hard to ignore, especially when the additional absorption of PCBM in the same frequency region is taken into account. Furthermore, since PCBM possesses a smaller average refractive index than P3HT ($n_{\text{P3HT}} = 2.22$, $n_{\text{PCBM}} = 1.35$),²⁴ the introduction of the PCBM molecules into P3HT layer would lead to a lower reflectance. This means that the light entering the samples is enhanced. After the absorption of the P3HT/PCBM film was measured, the sample was washed by spin-coating the pure DCM solvent and measured again. In this case, the PCBM absorption peak at 340 nm disappears and the absorption of

P3HT almost completely returns. This indicates that PCBM can easily penetrate and be removed from the P3HT layer. Therefore, there is a direct correlation between the P3HT absorption intensity and the diffusion of PCBM. Figure 2(b) shows the absorption spectra of the P3HT/PCBM films prepared using different concentration of the PCBM solution. As the concentration of the PCBM solution increases, the PCBM absorption peak at 340 nm increases, and the absorption intensity of P3HT between 450 and 650 nm gradually decreases. The increase in the PCBM absorption peak can be contributed to the increase of the amount of PCBM in the films.

As demonstrated by several groups,^{25,26} the PCBM molecules are miscible and mobile in disordered P3HT but not in the highly crystalline P3HT, especially when the motion of the polymer chain is suppressed at the room temperature. For the LE-BHJ film, if PCBM only penetrate into the original amorphous regions in the P3HT film, the order of the P3HT film should be maintained and the absorption intensity of P3HT should not change significantly. To determine the reason for the decrease in the P3HT absorption and the role that DCM played in the diffusion of the PCBM molecules, we compared the absorption and crystallinity of the P3HT films with and without the addition of DCM to the film. The P3HT film on quartz substrate was soaked in a quartz cuvette full of DCM solvent for absorption measurement and excessive DCM was dropped on the P3HT film for an immediately XRD testing. As shown in Figure 3(a), when the P3HT film was soaked in DCM, the shape of the absorption spectra changed and the absorption intensity decreased significantly. The P3HT absorption intensity is directly proportional to the P3HT chain packing and crystallinity.^{22,27} To quantitatively compare the order of the pristine P3HT film and the P3HT film that is soaked in DCM, the spectra were normalized according to the peak intensity at 520 nm [Figure 3 (b)]. It can be clearly seen that the peak intensity ratios of I_{558}/I_{520} and I_{602}/I_{520} both decrease when the film was soaked in DCM. This suggests that there is decreased stabilization of the P3HT chains and the decreased crystallinity.²² When

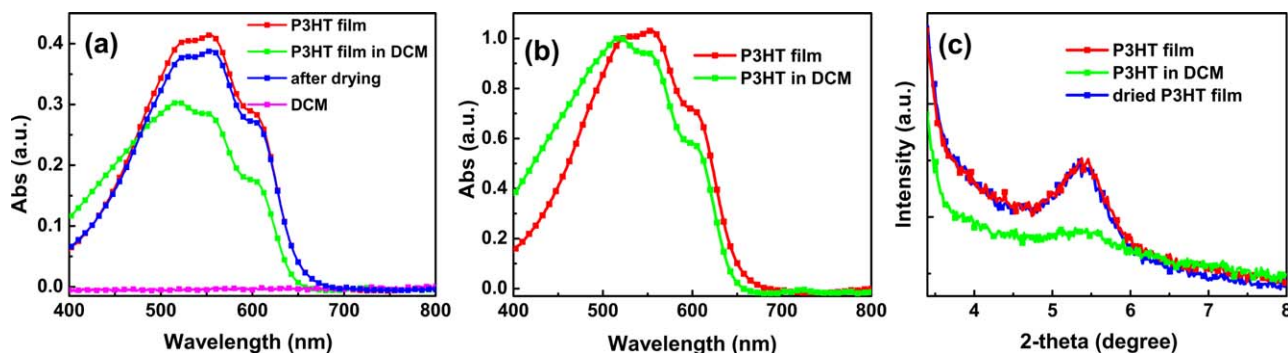


Figure 3. (a) The absorption spectra of the pure DCM solution, the P3HT film, the P3HT film in the DCM solution and the dried P3HT film. (b) The absorption spectra of the pristine P3HT film and the P3HT film in DCM, which are normalized according to the peak intensity at around 520 nm. (c) XRD patterns of the P3HT film, the P3HT film in DCM and the dried P3HT film. [Color figure can be viewed in the online issue, which is available at wileyonlinelibrary.com.]

the P3HT film was taken out of the DCM and dried, the absorption intensity of P3HT returned. This should be related to the self-reorganization of polymer.

The XRD profiles are shown in Figure 3(c). The pristine P3HT film exhibited an intense (1 0 0) diffraction peaks at $2\theta = 5.47^\circ$, which corresponds to the interchain spacing in P3HT associated with the interdigitated alkyl side chains.²⁸ The intensity of the XRD peak decreased dramatically when the P3HT film was soaked in DCM. After the DCM evaporated, the intensity of XRD peak returned. The XRD results follow the same trend as the absorption spectra. The existence of DCM disrupts the polymer chain packing and reduces the optical absorption. The disrupted chain packing of P3HT can be explained by the swelling of the P3HT film in which the DCM molecules fill the gaps between the polymer chains and enlarge the interchain distance. After drying, the DCM molecules evaporate from P3HT matrix and the polymer chains reorganize and repack. As a result, both the crystallinity and absorption recover after the deswelling process. We also measured the absorption spectra and XRD pattern of the P3HT film that was spin-coated with 150 μL of pure DCM. The results are shown

in Figure 4(a) and (b). There is no distinguishable change in the absorption spectra and XRD plots compared with that of the pristine P3HT film. This result is consistent with previous reports.¹⁰ However, it is insufficient to claim that DCM does not affect the order of the P3HT during the whole DCM spin-coating process. A quick swelling and self-recrystallizing process occurs.

On the basis of the results discussed above, we can propose a mechanism to explain the diffusion of the PCBM into the P3HT in the spin-coating process. The P3HT film spin-coated with pure DCM undergoes a swelling and deswelling process. Although the DCM disturbs some of the crystalline domains, the crystallinity of P3HT recovers after the evaporation of DCM. The different process of P3HT film spin-coated with the DCM solution of PCBM is that the PCBM molecules in the DCM solution are able to penetrate into the amorphous regions that are generated by the DCM solution. The PCBM molecules reside within the amorphous regions after DCM evaporates, and hinder the re-organization of the P3HT. As a result, the order and the optical absorption of the P3HT decrease after the deposition of PCBM layer.

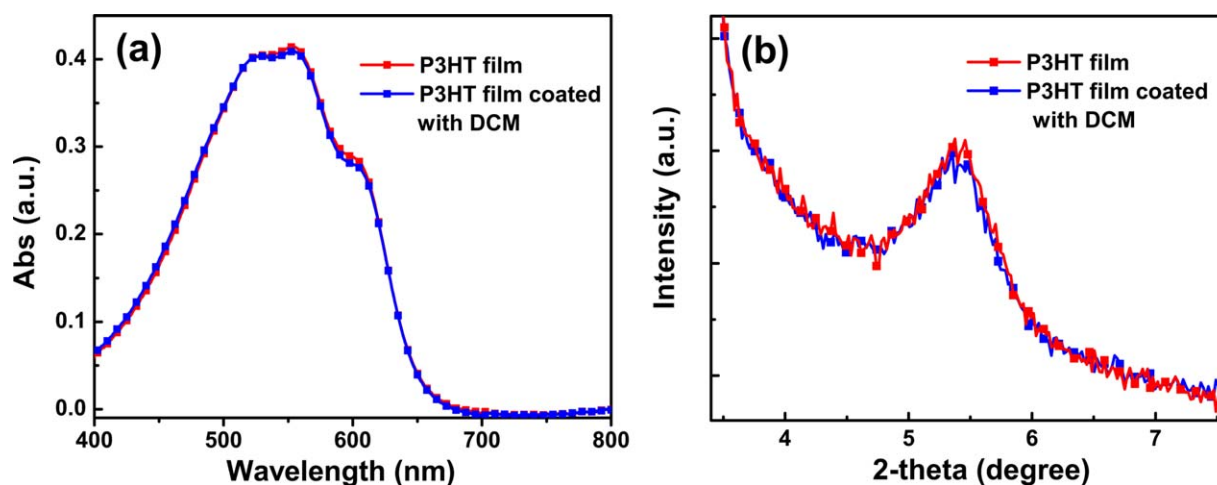


Figure 4. The absorption spectra (a) and XRD patterns (b) of the P3HT film and the P3HT film spin-coated with 150 μL of DCM. [Color figure can be viewed in the online issue, which is available at wileyonlinelibrary.com.]

CONCLUSIONS

In summary, we fabricated a P3HT/PCBM “bilayer” film with LE-BHJ structure by sequentially depositing of P3HT and PCBM from orthogonal solvents. PL spectra and J–V curves confirm the occurrence of substantial interdiffusion and mixing between P3HT and PCBM when the PCBM is spin-coated. A detailed study of steady-state absorption and XRD spectroscopy indicates that in spite of the insolubility of P3HT in DCM, DCM still can decrease the order of the P3HT and assist in the penetration of PCBM into the P3HT layer. After the evaporation of DCM, the PCBM hinders the self-reorganization of the P3HT, which gives rise to the decrease in the absorption intensity.

ACKNOWLEDGMENTS

This work was financially supported by the National Science Foundation for Distinguished Yong Scholars of China (61125505) and the National Natural Science Foundation of China (Grant Nos. 61377028, 61274063). The Fundamental Research Funds for the Central University 2014JBZ009.

REFERENCES

1. Thompson, B. C.; Frechét, J. M. J. *Angew. Chem. Int. Ed.* **2008**, *47*, 58.
2. Li, C.; Liu, M. Y.; Pschirer, N. G.; Baumgarten, M.; Mullen, K. *Chem. Rev.* **2010**, *110*, 6817.
3. Tang, C. W. *Appl. Phys. Lett.* **1986**, *48*, 183.
4. Wang, D. H.; Choi, D. G.; Lee, K. J.; Im, S. H.; Park, O. O.; Park, J. H. *Org. Electron.* **2010**, *11*, 1376.
5. Chen, D.; Liu, F.; Wang, C.; Nakahara, A.; Russell, T. P. *Nano Lett.* **2011**, *11*, 2071.
6. He, Z. C.; Zong, C.; Su, S.; Xu, M.; Wu, H.; Cao, Y. *Nat. Photon* **2012**, *6*, 591.
7. Samuele, L.; Tiziano, A.; Ellis, P.; Mark, H.; Jenny, N.; Macdonald, J. *Macromolecules* **2011**, *44*, 2725.
8. Li, G.; Shrotriya, V.; Huang, J.; Yao, Y.; Moriarty, T.; Emery, K.; Yang, Y. *Nat. Mater.* **2005**, *4*, 864.
9. Ma, W.; Yang, C.; Gong, X.; Lee, K.; Heeger, A. J. *Adv. Funct. Mater.* **2005**, *15*, 1617.
10. Ayzner, A. L.; Tassone, C. J.; Tolbert, S. H.; Schwartz, B. J. *J. Phys. Chem. C* **2009**, *113*, 20050.
11. Lee, K. H.; Schwenn, P. E.; Smith, A. R. G.; Cavaye, H.; Shaw, P. E.; James, M.; Krueger, K. B.; Gentle, I.; Meredith, P.; Burn, P. L. *Adv. Mater.* **2011**, *23*, 766.
12. Moon, J. S.; Takacs, C. J.; Sun, Y.; Heeger, A. J. *Nano Lett.* **2011**, *11*, 1036.
13. Rochester, C. W.; Mauger, S. A.; Moule, A. J. *J. Phys. Chem. C* **2012**, *116*, 7287.
14. Lee, K. H.; Zhang, Y.; Burn, P. L.; Gentle, J. R.; James, M.; Nelson, A.; Meredith, P. *J. Mater. Chem. C* **2013**, *1*, 2593.
15. Gevaerts, V. S.; Koster, J. A.; Wienk, M. M.; Janssen, R. J. *Appl. Mater. Interfaces* **2011**, *3*, 3252.
16. Zhang, G.; Huber, R.; Ferreira, A.; Boyd, S. D.; Luscombe, C. K.; Tolbert, S. H.; Schwartz, B. J. *J. Phys. Chem. C* **2014**, *118*, 18424.
17. Yang, B.; Yuan, Y. B.; Huang, J. S. *J. Phys. Chem. C* **2014**, *118*, 5196.
18. Wong, M. K.; Wong, K. Y. *Synth. Met.* **2013**, *170*, 1.
19. Lin, X.; Seok, J.; Yoon, S.; Kim, T.; Kim, B.; Kim, K. *Synth. Met.* **2014**, *196*, 145.
20. Hawks, S.; Aguirre, J.; Schelhas, L.; Thompson, R.; Huber, R.; Ferreira, A.; Zhang, G.; Herzing, A.; Tolbert, S. *J. Phys. Chem. C* **2014**, *118*, 17413.
21. Brown, P. J.; Thomas, D. S.; Kohler, A.; Wilson, J. S.; Kim, J. S.; Ramsdale, C. M.; Sirringhaus, H.; Friend, R. H. *Phys. Rev. B* **2003**, *67*, 064203.
22. Liu, J.; Shao, S.; Wang, H.; Zhao, K.; Xue, L.; Gao, X.; Xie, Z.; Han, Y. *Org. Electron.* **2010**, *11*, 775.
23. Shrotriya, V.; Yang, J.; Tseng, J.; Li, G.; Yang, Y. *Chem. Phys. Lett.* **2005**, *411*, 138.
24. Ai, X.; Beard, M. C.; Knutsen, K. P.; Shaheen, S. E.; Rumbles, G.; Ellingson, R. J. *J. Phys. Chem. B* **2006**, *110*, 25462.
25. Treat, N. D.; Brady, M. A.; Smith, G.; Toney, M. F.; Kramer, E. J.; Hawker, C. J.; Chabynyc, M. L. *Adv. Ener. Mater.* **2011**, *1*, 82.
26. Collins, B. A.; Gann, E.; Guignard, L.; McNeill, C. R.; Ade, H. *J. Phys. Chem. Lett.* **2010**, *1*, 3160.
27. Ng, A.; Liu, X.; Jim, W. Y.; Djuricic, A. B.; Lo, K. C.; Li, S. Y.; Chan, W. K. *J. Appl. Polym. Sci.* **2014**, *131*, 39776.
28. Kim, Y.; Cook, S.; Tuladhar, S. M.; Choulis, S. A.; Nelson, J.; Durrant, J. R.; Bradley, D. D. C.; Giles, M.; McCulloch, I.; Ha, C. S.; Ree, M. *Nat. Mater.* **2006**, *5*, 197.